Clinical Cancer Research

NKG2D-Dependent Antitumor Effects of Chemotherapy and Radiotherapy against Glioblastoma

Tobias Weiss[1], Hannah Schneider[1], Manuela Silginer[1], Alexander Steinle[2], Martin Pruschy[3], Bojan Polić[4], Michael Weller[1], and Patrick Roth[1]

Abstract

Purpose: NKG2D is a potent activating immune cell receptor, and glioma cells express the cognate ligands (NKG2DL). These ligands are inducible by cellular stress and temozolomide (TMZ) or irradiation (IR), the standard treatment of glioblastoma, could affect their expression. However, a role of NKG2DL for the efficacy of TMZ and IR has never been addressed.

Experimental Design: We assessed the effect of TMZ and IR on NKG2DL *in vitro* and *in vivo* in a variety of murine and human glioblastoma models, including glioma-initiating cells, and a cohort of paired glioblastoma samples from patients before and after therapy. Functional effects were studied with immune cell assays. The relevance of the NKG2D system for the efficacy of TMZ and IR was assessed *in vivo* in syngeneic orthotopic glioblastoma models with blocking antibodies and NKG2D knockout mice.

Results: TMZ or IR induced NKG2DL *in vitro* and *in vivo* in all glioblastoma models, and glioblastoma patient samples had increased levels of NKG2DL after therapy with TMZ and IR. This enhanced the immunogenicity of glioma cells in a NGK2D-dependent manner, was independent from cytotoxic or growth inhibitory effects, attenuated by O^6-methylguanine-DNA-methyltransferase (MGMT), and required the DNA damage response. The survival benefit afforded by TMZ or IR relied on an intact NKG2D system and was decreased upon inhibition of the NKG2D pathway.

Conclusions: The immune system may influence the activity of convential cancer treatments with particular importance of the NKG2D pathway in glioblastoma. Our data provide a rationale to combine NKG2D-based immunotherapies with TMZ and IR.
Clin Cancer Res; 24(4); 882–95. ©2017 AACR.

Introduction

Glioblastoma is the most common malignant primary brain tumor in adults with a dismal prognosis (1). The first-line treatment in patients below 70 years of age includes surgical resection as feasible, radiotherapy, and concomitant and maintenance chemotherapy with temozolomide (TMZ), an alkylating agent that induces DNA damage (2, 3). In addition to these treatment modalities, several promising immunotherapeutic approaches against glioblastoma are currently being evaluated (4, 5). These efforts are supported by the observation that glioma cells express molecules that allow for an interaction with cells of the immune system such as major histocompatibility complex (MHC) class I and class II molecules (6) as well as MHC class I–like ligands that bind to the activating immune cell receptor natural-killer group 2 member D (NKG2D; ref. 7). In humans, NKG2D ligands (NKG2DL) comprise the MHC class I–related chains (MIC) A and B (MICA, MICB) and the UL16 binding proteins (ULBP) 1–6 (8). These ligands are expressed on human glioma cells *in vitro* (9) and *in vivo* (10) as well as on glioma-initiating cells (GIC), a subpopulation of cells with stem cell properties (11, 12). In mice, NKG2DL comprise the retinoic acid early inducible-1 (RAE-1) proteins, members of the H60 family (H60a, H60b, and H60c) and the murine UL16-binding protein like transcript-1 (MULT-1), which are also expressed by mouse glioma cells (9, 13). All NKG2DL bind to the NKG2D receptor, which is one of the major activating receptors on natural killer (NK) cells (8). In addition to NK cells, this receptor is constitutively expressed on NKT cells, αβ CD8 T cells, and γδ T cells (8, 14). Furthermore, its expression is induced on CD4 T cells by TNF-α and IL15 (15, 16). However, various glioma-derived humoral and cellular immunosuppressive mechanisms preclude an efficient antitumor immune response, including the expression of transforming growth factor (TGF)-β (17), prostaglandin E2 (PGE2; ref. 18), IL10 (19), growth and differentiation factor (GDF)-15 (20), lectin-like transcript 1 (LLT1; ref. 21), indoleamine 2,3-dioxygenase (IDO; ref. 22), programmed death ligand 1 (PD-L1; ref. 23), as well as the presence of immunosuppressive regulatory T cells (Tregs; ref. 24) and M2-polarized microglia (25). Enhancing the immunogenicity of glioma cells may be achieved either by inhibition of these immunosuppressive mechanisms (26) or by promoting immune activating signals such as the NKG2DL (27). Because various cellular stress stimuli including malignant transformation of cells

[1]Department of Neurology and Brain Tumor Center, University Hospital Zurich and University of Zurich, Switzerland. [2]Institute for Molecular Medicine, University of Frankfurt, Germany. [3]Department of Radiation Oncology, University Hospital Zurich and University of Zurich, Switzerland. [4]Department of Histology and Embryology, Faculty of Medicine, University of Rijeka, Croatia.

Note: Supplementary data for this article are available at Clinical Cancer Research Online (http://clincancerres.aacrjournals.org/).

Corresponding Author: Patrick Roth, Department of Neurology, University Hospital Zurich, Frauenklinikstrasse 26, 8091 Zurich, Switzerland. Phone: 41-44-255-5511; Fax: 41-44-255-4380; E-mail: patrick.roth@usz.ch

doi: 10.1158/1078-0432.CCR-17-1766

Translational Relevance

Temozolomide and radiotherapy are the adjuvant standard of care for patients with glioblastoma. This article demonstrates an unprecedented role of the NKG2D-dependent immune pathway for the efficacy of these anticancer therapies against glioblastoma. Both treatment modalities induce immune-stimulatory NKG2D ligands also in unfavorable but clinically relevant settings of *MGMT* overexpression, TMZ resistance, and at tumor recurrence. This promotes the role of the NKG2D system as an attractive immunotherapeutic target in glioblastoma at primary diagnosis and at recurrence. Furthermore, it provides a strong rationale for future combination studies of conventional radiochemotherapy and NKG2D-based immunotherapy.

or DNA damage can induce NKG2DL (8), we explored whether TMZ or irradiation (IR) as part of the standard treatment for glioblastoma increase NKG2DL levels on glioma cells and whether this promotes their immunogenicity. We also defined the molecular mechanisms underlying the TMZ- and IR-induced NKG2DL expression in glioma cells. Finally, we investigated the significance of the NKG2D system for the survival benefit gained with TMZ and IR in several immunocompetent mouse glioma models.

Materials and Methods

Cells and materials

The human glioma cell lines LN-18 and LN-229 were kindly provided by Dr. N. de Tribolet (Centre Hospitalier Universitaire Vaudois, Lausanne, Switzerland). LN-229-R cells were generated by repetitive exposure to TMZ resulting in a shift of the EC_{50} (28). Generation of LNT-229_MGMT and LNT-229_neo (29) and LN-18_shMGMT and LN-18_puro cells (30) has been described. SMA-560 glioma cells were obtained from Dr. D. Bigner (Duke University Medical Center, Durham, NC) and GL-261 were obtained from the National Cancer Institute (Frederick, MD). SMA-560_Turbo650 and GL-261_NirFP were created by lentiviral transduction of GL-261 and SMA-560 cells with plasmids encoding near-infrared fluorescent proteins Turbo650 and NirFP (Evrogen) and selection by fluorescence-activated cell sorting (FACS). Adherent cell lines were maintained in Dulbecco's Modified Eagle Medium (DMEM; Invitrogen), containing 2 mmol/L L-glutamine (Gibco Life Technologies), and 10% fetal calf serum (FCS; Biochrom KG). The GIC cell lines S-24 and ZH-305 were generated from human glioblastoma patient specimens (31). After tumor removal, tissue was dissociated using a papain system and a gentleMACS Dissociator (Miltenyi Biotec). These cells were then maintained as suspension cultures in Neurobasal Medium with B-27 supplement (20 μL/mL) and glutamax (10 μl/mL) from Invitrogen and fibroblast growth factor (FGF)-2, epidermal growth factor (EGF; 20 ng/mL each; Peprotech) and heparin (32 IE/mL; Ratiopharm). All cell lines were routinely tested for *Mycoplasma* using PCR (last test in December 2016). For all experiments described herein, the adherent cells were allowed to attach over a 24-hour period. Subsequently, the experiments were carried out in serum-free medium. KU-60019 (Selleckchem) is a potent and specific ataxia-telangiectasia mutated (ATM) inhibitor, and concentrations < 1.5 μmol/L ensure specificity for ATM. TMZ, kindly provided by Schering-Plough, was prepared in stock solutions (100 mmol/L) in dimethylsulfoxide (DMSO). N-(2-chloroethyl)-N′-cyclohexyl-N-nitrosourea (CCNU) was kindly provided by Medac. Cells were irradiated using a cobalt-60 source (Sulzer), and for different fractionations the approximative biological effective dose and dose per fraction according to the linear quadratic model (32) were determined using the R package DVHmetrics (https://cran.r-project.org/web/packages/DVHmetrics/index.html) under the assumption of an α/β ratio of 10 for human glioma cell lines. Thiazolyl blue tetrazolium bromide (MTT) was obtained from AxonLAb.

Antibodies and flow cytometry

The following monoclonal antibodies (mAb) were used for the assessment of cell surface expression of MICA, MICB, ULBP2, ULBP3, RAE-1, MULT-1, H60 or blocking of NKG2D: MICA (AMO1, mouse IgG1), MICB (BMO1, mouse IgG1), ULBP2 (BUMO1, mouse IgG1), and ULBP3 (CUMO3, mouse IgG1). Their generation has been described previously (33). RAE-1_FITC and MULT-1_PE and blocking anti-human NKG2D (clone 149810) were obtained from R&D Systems Europe. H60_PerCP was obtained from Novus Biologicals. Blocking but not depleting anti-mouse NKG2D (clone C7) was obtained from eBioscience. As controls, we used isotype-matched antibodies from Sigma-Aldrich. The PE-conjugated goat anti-mouse IgG from Dako was used as secondary antibody where appropriate. Cells were detached with Accutase (Life Technologies), preincubated in phosphate-buffered saline (PBS) with 2% FCS, and stained with specific mAbs (10 μg/mL) or matched mouse Ig isotype for 30 minutes on ice, followed by incubation with PE-conjugated secondary antibody for 30 minutes where appropriate. After washing, flow cytometric analyses were performed using a BD FACSVerse Analyzer (BD). In case of intracellular staining for $ATM^{ser1981}$, Fix/Perm Buffer Set from BioLegend was used. For flow cytometric assessment of tumor-infiltrating lymphocytes, live/dead staining with FVS 510, anti-CD3_ PerCP-Cy5.5, anti-CD4_FITC, anti-CD8_APC-H7, anti-NKp46_PE, anti-IFNγ_APC, and anti-TCRγ/δ_BV421 from BioLegend were used. Specific fluorescence indexes (SFI) were calculated by dividing median fluorescence obtained with the specific antibody by median fluorescence obtained with isotype control antibody. For *in vivo* experiments, fluorescence intensity was expressed as median fluorescence intensity. Data were analyzed with FlowJo software (TreeStar).

Immune cell cytotoxicity assay

We used a flow cytometry-based cytotoxicity assay to determine immune-mediated glioma cell lysis (34). Specific lysis was expressed as percentage of cell death of the PKH-26 labeled targets. Percentage of target cell lysis was corrected for spontaneous background lysis by subtracting the percentage of dead cells in control samples (targets alone) from the percentage of dead cells within the test samples. As effector cells, we used either splenocytes isolated from mice, human NK cells isolated from PBMC by negative selection using an NK cell isolation kit (Miltenyi Biotec) or NKL cells obtained from M.J. Robertson (Indiana University School of Medicine, Indianapolis, IA). For blocking experiments, NKL cells were preincubated for 2 hours at 4°C with anti-NKG2D or IgG1 isotype control, and the antibody was also present during the

coincubation of target and effector cells. All experiments were done in triplicates.

Real-time PCR

Total RNA was isolated using the NucleoSpin RNA II system from Macherey-Nagel and cDNA was prepared using the iScript cDNA Synthesis Kit from Bio-Rad Laboratories AG. For real-time PCR, gene expression was measured in an ABI Prism 7000 Sequence Detection System (Applied Biosystems) with SYBR Green Master Mix (Thermo Fisher Scientific) and primers (Microsynth AG) at optimized concentrations. Primers for *MICA*, *MICB*, *ULBP2*, and *ULBP3* have been published (35). Primers used to detect murine NKG2DL were *RAE-1* forward 5′-TTTGGGAGCACAACCACAGAT-3′, reverse 5′-TAAAGTTGGCGGGCTGAAAGA-3′, *MULT-1* forward 5′-CTGCCAGTAACAAGGTCCTTTC-3′, reverse 5′-GCTGTTCCTATGAGCACCAATG-3′, *H60a* forward 5′-CTGAGCTATCTGGGGACCATAC-3′, and reverse 5′-AGTCTTTCCATTCACTGAGCAC-3′. As reference gene, we used human *HPRT1*: forward 5′-TGAGGATTTGGAAAGGGTGT-3′, reverse 5′-GAGCACACAGAGGGCTACAA-3′, and mouse *HPRT1*: forward 5′-TTGCTGACCTGCTGGATTAC-3′, reverse 5′-TTTATGTCCCCCGTTGACTG-3′ respectively. The conditions were 40 cycles at 95°C/15 seconds and 60°C/1 minute. Standard curves were generated for each gene. Relative quantification of gene expression was determined by comparison of threshold values. All results were normalized to *HPRT1* and calculated with the ΔCTT method for relative quantification.

Determination of cytotoxicity, acute cytostatic or clonogenic effects

For determination of cytotoxicity, 5×10^3 cells were seeded per well in 96-well plates, allowed to attach for 24 hours (adherent cells) and irradiated or exposed to TMZ, CCNU, or staurosporine as indicated for 72 hours in serum-free medium. Percentage of living cells was determined by flow cytometry after live/dead staining with Zombie Aqua Fixable Viability Kit (BioLegend). For acute growth inhibition assays, we used the same experimental setting but either crystal violet staining (for adherent cells) or MTT (for suspension cells) as read-out. Clonogenic survival assays were performed by seeding 10^2 cells per well in 96-well plates. After 24 hours, the cells were irradiated or exposed to TMZ, CCNU, or staurosporine as indicated for 24 hours in serum-free medium, followed by observation for 20 days. As readout methods, we again used either crystal violet staining or MTT.

Immunoblot analyses

For the detection of proteins in cell lysates, cells were lysed and processed as previously described (28). Thirty micrograms of protein was used per lane and visualization of protein bands was accomplished using horseradish peroxidase (HRP)-coupled secondary antibodies (Sigma-Aldrich) and enhanced chemiluminescence (Pierce/Thermo Fisher).

Immunofluorescence

Cells were cultured in chamber slides with polystyrene-treated glass (BD Biosciences), fixed with 4% paraformaldehyde and permeabilized with 0.5% Triton X-100 (Sigma-Aldrich). Blocking with 3% FCS was followed by incubation with anti-ATM protein kinase pS1981 monoclonal antibody (Rockland; diluted 1:100) overnight at 4°C. Donkey anti-mouse IgG Alexa Fluor 488–labeled secondary antibody (Life Technologies) was used at 1:200. Slides were mounted in Vectashield Mounting Media with DAPI, and images were acquired by using a Leica TCS SP5 confocal microscope.

Mice and animal experiments

All experiments were done in accordance with the guidelines of the Swiss federal law on animal protection and were approved by the cantonal veterinary office. C57BL/6 mice were purchased from Charles River Laboratories. VM/Dk mice were bred in pathogen-free facilities at the University of Zurich. NKG2D$^{-/-}$ mice have been previously described (36) and were kindly provided by D. H. Busch (Munich, Germany). Mice of 6 to 12 weeks of age were used in all experiments in groups of 7 to 10 mice. For intracranial tumor implantation, SMA-560 cells (5×10^3) or GL-261 cells (2×10^4) were stereotactically implanted into the right striatum at day 0. Mice were observed daily and sacrificed as indicated or in the survival experiments when developing neurologic symptoms. If indicated, local cranial radiotherapy with a single dose of 12 Gy was performed at day 10 after tumor implantation using a Gulmay 200 kV X-ray unit at 1 Gy/minute at room temperature. If indicated, mice received TMZ (10 mg/kg/day) per oral gavage from days 7 to 11 after tumor implantation. MRI was performed with a 4.7 T small animal magnetic resonance imager (Pharmascan; Bruker Biospin) at day 13 after tumor implantation. Coronal T2-weighted images were acquired using Paravision 6.0 (Bruker BioSpin). Mean ± SD of the tumor volume in mm^3 from 5 mice/group were determined by the formula (length × width × depth)/2.

For *in vivo* blockade of NKG2D signaling, mice were injected i.p. with 100 μg of the blocking but not depleting anti-NKG2D antibody (clone C7; ref. 37) or with isotype control in PBS. Antibodies were given either 1 day before and 1 day after tumor implantation or at days 6 and 7 after tumor implantation and were reinjected every 7 days until the mice were sacrificed. Time of antibody administration is indicated in the figure legends.

Isolation of orthotopic tumor cells was performed on day 12 after tumor implantation. Brains were harvested after transcardial perfusion with ice-cold PBS to remove all circulating leukocytes from the CNS. Tumor cells were separated from myelin and red blood cells using a Percoll gradient suspension (Sigma-Aldrich). Cells were washed with PBS and stained with Zombie Aqua Fixable Viability Kit and fluoroconjugated antibodies specific to indicated cell surface markers for flow cytometry.

Tissue microarray of patient samples

Studies were approved by the Institutional Review Board (KEK-StV-Nr.19/08), and informed consent was received prior to inclusion to the study. Twenty-one pairs of primary (before chemoradiation) and recurrent glioblastoma (variable time points after chemoradiation) specimens from patients who underwent brain tumor resection between 2000 and 2014 at the Department of Neurosurgery, University Hospital Zurich (Zurich, Switzerland) were collected. Immunohistochemistry was performed as described (31) using anti-MICA, anti-MICB, anti-ULBP2, or anti-ULBP3 antibodies from Sino Biological (Lucerna-Chem AG) or antiprogrammed death-ligand 1 (PD-L1) from Cell Signaling Technology. Images were analyzed in an unsupervised and blinded fashion using TMARKER, a software toolkit for histopathologic staining estimation (38).

Statistical analysis

Data were presented as means ± SD. Experiments were repeated at least three times, if not indicated differently. Viability and acute and clonogenic cell growth studies were performed at least in triplicates. Statistical analyses were performed in GraphPad Prism using multiple two-tailed Student *t* tests and correction for multiple comparisons using the Holm–Sidak method. For analysis of tissue microarray data, we used Wilcoxon matched-pairs signed rank test. For analysis of heterogeneity of immunohistochemically stained NKG2DL, we calculated the intraclass correlation coefficient (ICC; ref. 39) as a statistical measure to assess staining variation for 2 tissue cores from each tumor sample by using the R-package ICC (https://cran.r-project.org/web/packages/ICC/index.html). Kaplan–Meier survival analysis was performed to assess survival differences among the treatment groups and *P* values were calculated with the Gehan–Breslow–Wilcoxon test. Throughout all figures, significance was concluded at *, $P < 0.05$ and **, $P < 0.01$.

Results

TMZ induces NKG2DL expression in glioma cells independent from cytotoxic and growth-inhibitory effects

Exposure of glioma cells to TMZ has growth-inhibitory as well as cytotoxic effects. To define the sensitivity of LN-18 and LN-229 cells to TMZ, we treated these cells with a broad range of TMZ concentrations and determined cell death, acute growth inhibition, and clonogenic cell survival (Fig. 1A). Because NKG2DL are upregulated in response to various stress stimuli, we explored in a next step whether TMZ induces the expression of NKG2DL in these cells. We observed an induction of several NKG2DL on mRNA and protein cell surface level over a wide concentration range (Fig. 1A; Supplementary Fig. S1A–S1B) including low concentrations with minor cytotoxic and growth-inhibitory effects as well as clinically relevant concentrations around plasma levels of 30 to 80 μmol/L of TMZ that are achieved in human patients (40). To evaluate the effect on other activating immune cell receptor ligand systems, we assessed CD112 and CD155 as ligands of the human DNAX accessory molecule-1 (DNAM-1, CD226) activating immune cell receptor. In contrast to NKG2DL, the cell surface expression of CD112 and CD155 was unaffected by TMZ (Supplementary Fig. S1C). Next, we examined the effect of TMZ on NKG2DL expression in GIC, a subpopulation of glioma cells with stem-like properties that are associated with resistance to chemotherapy and irradiation (41). S-24 cells were relatively resistant to TMZ with an EC_{50} value of 267 μmol/L in clonogenic survival assays, whereas ZH-305 cells were more sensitive with an EC_{50} of 7.3 μmol/L (Fig. 1B). TMZ induced several NKG2DL on mRNA and cell surface protein levels in both GIC lines. Again, there was no induction of DNAM-1 ligands (Supplementary Fig. S1D). Furthermore, we determined the expression of NKG2DL on mouse glioma cells and their induction by TMZ. GL-261 and SMA-560 cells differed in their sensitivity to TMZ. The EC_{50} for clonogenic cell survival was ≈50 μmol/L for GL-261 and >500 μmol/L for SMA-560 (Fig. 1C). Similar to human cells, exposure to TMZ resulted in an upregulation of NKG2DL in both murine glioma cell models. H60a is not expressed in C57BL/6 mice and the syngeneic GL-261 cells (42) and was therefore not detected in this cell line.

To corroborate our findings that the upregulation of NKG2DL is not a general response pattern of glioma cells to cell death induction but rather a specific response to alkylating chemotherapy, we exposed LN-18 and LN-229 cells to different concentrations of staurosporine. Despite its strong effect on glioma cell viability, none of the NKG2DL was upregulated by staurosporine (Supplementary Fig. S1E). However, CCNU, another alkylating agent commonly used in patients with recurrent glioblastoma (43) also induced NKG2DL already at low concentrations, close to those typically achieved in the plasma of patients (3.4–3.8 μmol/L; ref. 44; Supplementary Fig. S1F).

Irradiation induces NKG2DL in human and mouse glioma cells independent from cytotoxic and cytostatic effects

Because radiotherapy belongs to the standard of care for glioma patients, we also assessed the effect of IR on NKG2DL expression in different glioma models. LN-18 cells were more sensitive to irradiation than LN-229 cells with an EC_{50} value of 4 vs. 11 Gy in clonogenic survival assays. In both cell lines, IR induced the expression of several NKG2DL on mRNA and cell surface protein level (Fig. 2A). The induction of NKG2DL cell surface expression following IR was also confirmed when different fractionation schemes were applied (Supplementary Fig. S2A). Consistent with the TMZ data, there was no induction of DNAM-1 ligands upon irradiation (Supplementary Fig. S2B). In S-24 and ZH-305 GIC, irradiation had minor cytotoxic effects with an EC_{50} value of > 20 Gy but clear effects on clonogenic survival with EC_{50} values ≈ 5 Gy. A clinically relevant single fraction in the range of 2 to 4 Gy increased NKG2DL mRNA and cell surface protein levels (Fig. 2B).

We also confirmed the irradiation-mediated induction of NKG2DL in GL-261 and SMA-560 mouse glioma cells. In both cell lines, irradiation upregulated NKG2DL on the mRNA as well as on cell surface protein level (Fig. 2C).

TMZ- but not irradiation-mediated NKG2DL induction is modulated by MGMT and both depend on ATM signaling

MGMT promoter methylation predicts benefit from alkylating chemotherapy with TMZ in glioblastoma. To explore whether the TMZ-mediated induction of NKG2DL is influenced by MGMT, we used subcell lines of LN-18 with a stably silenced *MGMT* gene (30) or LNT-229 cells that stably overexpress *MGMT* (29). The modulation of *MGMT* expression affected the sensitivity to TMZ (Fig. 3A), but not to IR (Supplementary Fig. S3A). Furthermore, *MGMT* expression significantly decreased TMZ-mediated NKG2DL induction. This was demonstrated by an increased NKG2DL induction upon shRNA-mediated *MGMT* silencing in LN-18 glioma cells that naturally express *MGMT* and a diminished NKG2DL induction in *MGMT*-overexpressing LNT-229 cells compared with *MGMT*-deficient wild-type LN-229 cells (Fig. 3B). The IR-mediated upregulation of NKG2DL was unaffected by the MGMT status (Supplementary Fig. S3B). Glioma cells can also acquire resistance to TMZ independent from MGMT expression. Mechanistically, this is linked, amongst others, to the downregulation of DNA mismatch–repair proteins (28). Because this acquired resistance is a challenge in clinical practice that needs alternative treatment options, we assessed the induction of potentially immune-activating NKG2DL in a glioma cell line with acquired TMZ resistance (28). Also in these cells, TMZ or IR induced the cell surface protein level of NKG2DL. The same effect was observed after IR (Supplementary Fig. S3C–S3D).

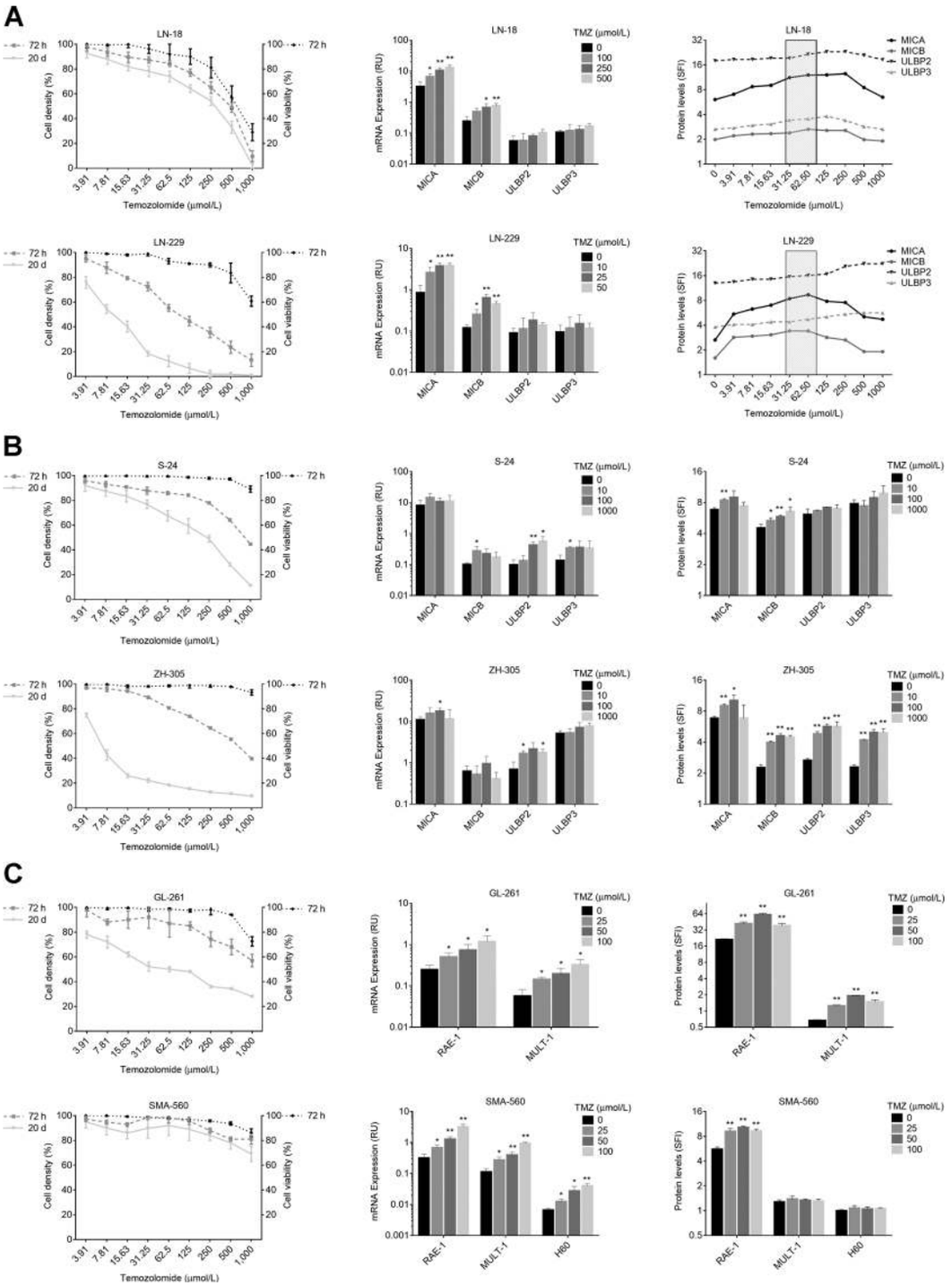

Figure 1.

TMZ induces NKG2DL in human and mouse glioma cells including human GIC independent from cell death and growth inhibition. **A,** LN-18 or LN-229 glioma cells were exposed to different concentrations of TMZ or DMSO control. Viability was assessed by live/dead staining at 72 hours (black dotted line), cytostatic effects were detected by crystal violet staining at 72 hours and 20 days (gray dashed and straight lines; left). Transcripts for MICA, MICB, ULBP2, or ULBP3 were assessed by real-time PCR after 48 hours (middle). Data represent mean values ± SD from 3 independent experiments (*, $P < 0.05$; **, $P < 0.01$). NKG2DL protein levels at the cell surface were determined by flow cytometry following exposure to TMZ or DMSO control for 72 hours (right). Data are presented as SFI and mean values ± SD from 3 independent experiments are shown (*, $P < 0.05$; **, $P < 0.01$). Gray areas represent TMZ plasma levels achieved in patients. **B** and **C,** S-24 or ZH-305 glioma-initiating cell lines (**B**) and GL-261 or SMA-560 mouse glioma cells (**C**) were treated as indicated and human or murine NKG2DL were analyzed as in A.

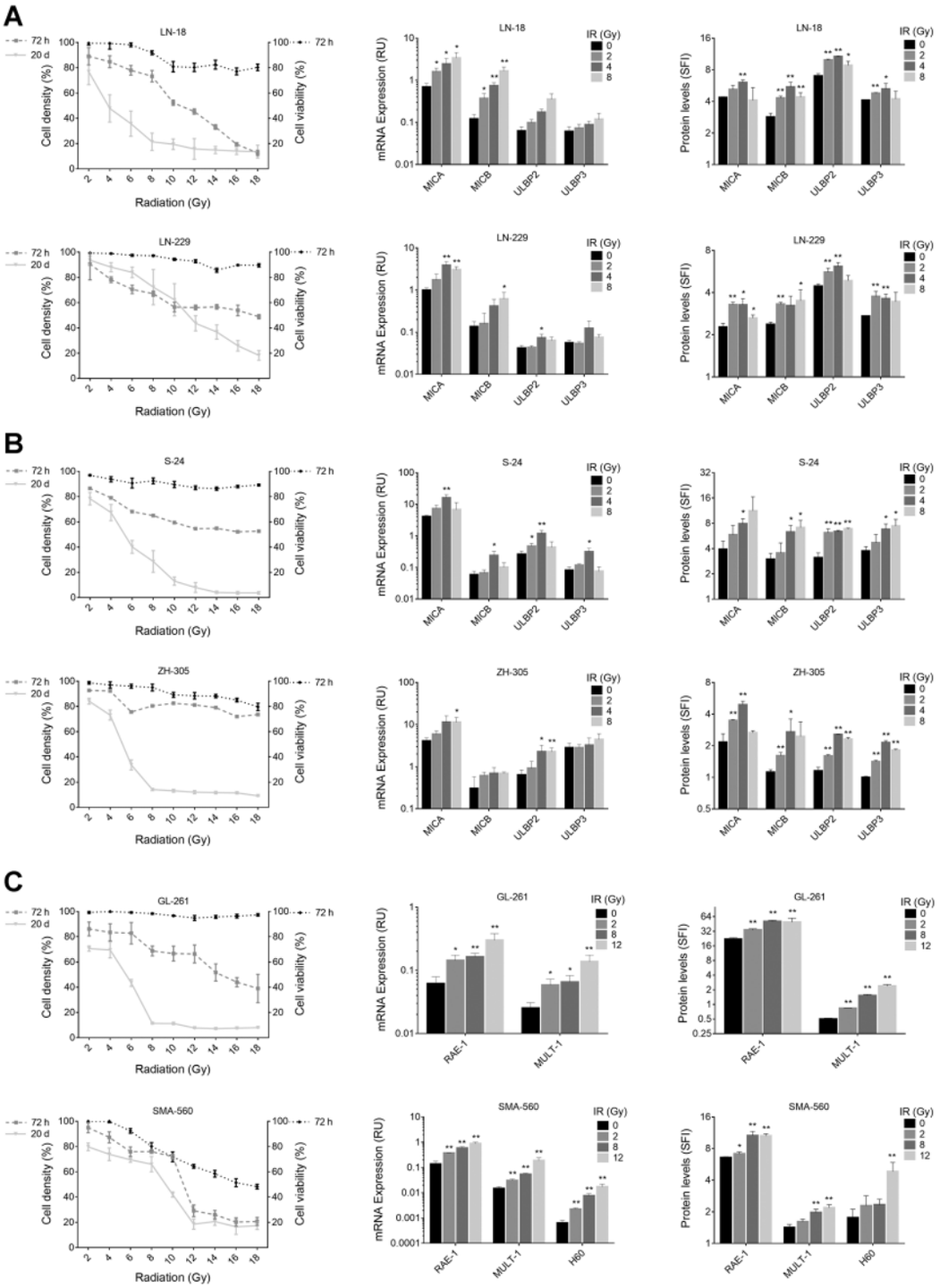

Figure 2.

IR induces NKG2DL in human and mouse glioma cells independent from cell death and cell growth inhibition. **A,** LN-18 or LN-229 glioma cells were irradiated with different doses of gamma irradiation. Viability was assessed by live/dead staining (black dotted line), cytostatic effects were detected by crystal violet staining (gray dashed and straight lines; left). Transcripts (MICA, MICB, ULBP2, or ULBP3) were assessed by real-time PCR after 48 hours (middle). Data represent mean values ± SD from independent experiments (*, $P < 0.05$; **, $P < 0.01$). NKG2DL protein levels at the cell surface were determined by flow cytometry 72 hours after IR (right). Data are presented as SFI, and mean values ± SD from 3 independent experiments are shown (*, $P < 0.05$; **, $P < 0.01$). **B** and **C,** S-24 or ZH-305 glioma-initiating cell lines (**B**) and GL-261 or SMA-560 mouse glioma cells (**C**) were irradiated as indicated and human or mouse NKG2DL were assessed as in **A**.

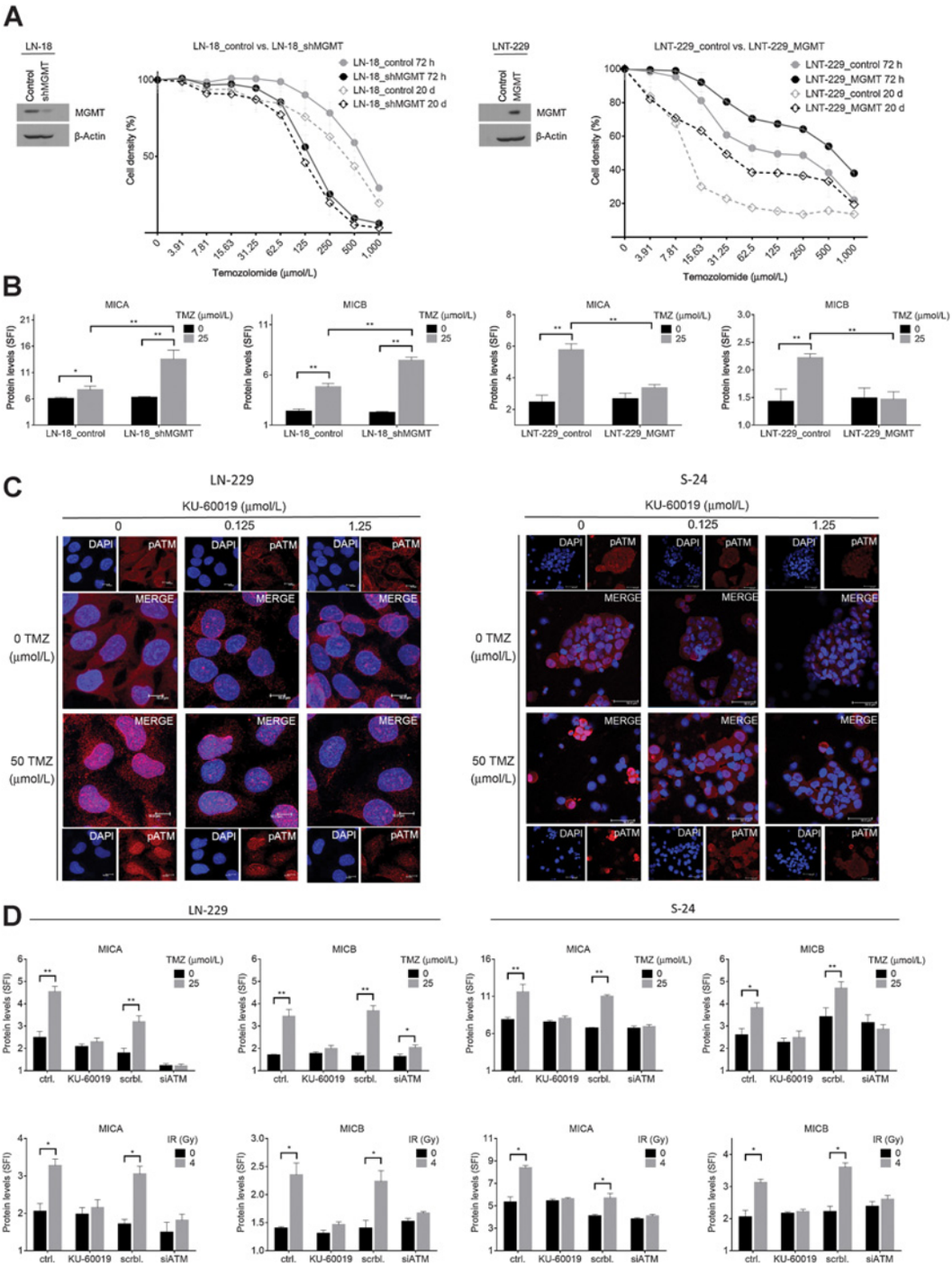

Figure 3.

NKG2DL induction is modulated by MGMT and depends on ATM. **A,** Whole cell lysates of LN-18_control or LN18_shMGMT cells and LN-229_control or LN-229_MGMT were assessed by immunoblot for MGMT protein levels. Beta-actin was used as a control. Acute cytostatic and clonogenic effects after exposure to TMZ were determined by crystal violet staining at the indicated time points. **B,** The cells were exposed to TMZ, and cell surface expression of MICA and MICB was determined after 72 hours by flow cytometry. Data are presented as SFI and mean ± SD of 3 independent experiments is shown (*, $P < 0.05$; **, $P < 0.01$). **C,** LN-229 (left) or S-24 (right) cells were treated with KU-60019 or DMSO 4 hours prior to TMZ exposure. Immunofluorescence images were acquired following $pATM^{Ser1981}$ staining (red). Nuclei are stained with DAPI (blue). **D,** LN-229 (left) or S-24 (right) were exposed to TMZ (top row) or IR (bottom) after ATM inhibition using KU-60019 or siRNA-mediated gene silencing. MICA and MICB cell surface expression were determined by flow cytometry. Data are presented as SFI, and mean values ± SD from 2 independent experiments are shown (*, $P < 0.05$; **, $P < 0.01$).

To elucidate the molecular mechanisms mediating the treatment-induced NKG2DL induction in glioma cells, we assessed the ATM pathway as part of the DNA damage response to genotoxic stress induced by TMZ (45). In LN-229 and S-24 cells, we detected an increase of active phospho-ATM^{Ser1981} upon exposure to TMZ (Fig. 3C). Inhibition of ATM using RNA interference (Supplementary Fig. S3E) or KU-60019, a specific ATM inhibitor that inhibited ATM at 1.25 μmol/L with little toxicity (Supplementary Fig. S3F), abrogated the TMZ-induced upregulation of MICA and MICB in LN-229, S-24 cells (Fig. 3D). We confirmed this also for ZH-305 cells (Supplementary Fig. S3G). Furthermore, we observed this ATM dependency also for irradiation-mediated NKG2DL induction (Fig. 3D; Supplementary Fig. S3G).

Exposure to TMZ and IR promotes glioma cell immunogenicity in a NKG2D-dependent manner

To investigate functional effects of the TMZ- or RT-induced NKG2DL induction, we performed cytotoxicity assays using polyclonal human NK cells or NKL cells (46) as immune effectors. Preexposure of LN-229 or S-24 cells to TMZ resulted in an enhanced immune cell–mediated cytolysis (Fig. 4A; Supplementary Fig. S4A). In contrast, exposure of *MGMT*-overexpressing LNT-229 cells to TMZ at the same concentrations did not enhance immune cell–mediated cytolysis (Supplementary Fig. S4B). Preincubation of effector cells with blocking but not depleting anti-NKG2D antibodies abrogated the TMZ-induced glioma cell susceptibility to immune cell killing (Fig. 4A). Similarly, LN-229 or S-24 cells that were preirradiated with 2 Gy were more susceptible to immune cell–mediated cytolysis in an NKG2D-dependent manner (Fig. 4B).

NKG2DL levels are increased *in vivo* in syngeneic glioma models following treatment with TMZ or IR as well as in human glioblastoma following radiochemotherapy

To study the effect of TMZ and irradiation on glioma-associated NKG2DL *in vivo*, we generated GL-261_niRP and SMA-560_TurboFP650 mouse glioma cells, which stably express near-infrared fluorescent proteins and which are syngeneic to C57BL/6 or VM/Dk mice. This allowed for the detection of these cells by flow cytometry (Fig. 5A) and the specific assessment of NKG2DL protein levels on the cell surface *ex vivo*. After orthotopic tumor cell injection, we treated mice either with a single dose of local IR at day 10 or with TMZ per oral gavage for 5 consecutive days starting at day 7 after tumor cell inoculation. At day 12, mice were euthanized, and the tumors were explanted. TMZ and irradiation led to an upregulation of NKG2DL in both orthotopic murine glioma cell models with a more pronounced effect in the SMA-560 model (Fig. 5A).

To study the effect of chemo- and radiotherapy on glioma-associated NKG2DL in human glioblastoma patients, we created a tissue microarray (TMA) encompassing 21 paired formalin-fixed samples of human glioblastoma specimens obtained before and after treatment with TMZ and/or radiotherapy. From 9 of these paired samples, we could also isolate RNA. Compared with basal expression, we detected increased levels of several NKG2DL on mRNA as well as on cell surface protein level after treatment with TMZ or IR or both (Fig. 5B). Based on 2 cores from each tumor, we found a heterogeneous expression of NKG2DL within tumors, particularly for ULBP2 and ULBP3 (Supplementary Fig. S5A). We did not observe correlations between NKG2DL and survival or NKG2DL and the immunosuppressive ligand PD-L1 in this small patient population. There were also no significant differences in PD-L1 expression between primary and recurrent human glioblastoma samples (Supplementary Fig. S5B–S5D).

The NKG2D system contributes to the therapeutic effects of TMZ and irradiation in glioma

Finally, we asked whether the NKG2D system plays any role for the survival benefit gained from TMZ or irradiation in murine glioma models. We inhibited the NKG2D system in fully immune-competent, orthotopic SMA-560 glioma-bearing mice by repetitive intraperitoneal injections of a blocking but not depleting anti-NKG2D antibody (37). Its biological activity reflecting target inhibition was verified by decreased *ex vivo* cytolysis of SMA-560 cells upon TMZ exposure or irradiation by immune effector cells isolated from anti–NKG2D-treated mice (Supplementary Fig. S6A). At the treatment schedules used, either IR or TMZ prolonged survival, but this effect was more prominent for IR. Administration of the anti-NKG2D antibody abrogated the survival benefit conferred by TMZ and attenuated the IR-mediated survival benefit in SMA-560 glioma-bearing mice (Fig. 6A). This NKG2D-dependent effect of TMZ or IR in SMA-560 glioma-bearing mice was also present when the anti-NKG2D antibody was administered at days 6 and 7 post tumor implantation when tumors had already been established (Supplementary Fig. S6B). To confirm the importance of an intact NKG2D system for the efficacy of TMZ and IR in glioma in a second syngeneic setting, we used NKG2D knockout (NKG2D$^{-/-}$) mice as an even more robust model. These mice were treated with the same regimen of TMZ or IR. In addition, we also included the combination of both treatments, reflecting the current standard of care for human glioblastoma patients. There was no difference in median survival of glioma-bearing NKG2D$^{-/-}$ or NKG2D-intact mice when no treatment was administered. TMZ or irradiation prolonged the median survival of GL-261 tumor–bearing mice and the combination of both therapies further increased the survival (Fig. 6B). However, the survival gain conferred by TMZ, irradiation, or the combination of both was significantly reduced in NKG2D$^{-/-}$ mice (Fig. 6B). The survival data were corroborated by MRI. At day 6 post tumor implantation, we could not clearly delineate the tumor due to superimposing post-surgery alterations, but at day 13 post tumor implantation, we observed reduced activity of the antitumor treatments with regard to tumor growth in NKG2D-deficient mice (Fig. 6C; Supplementary Fig. S6C). Finally, we analyzed tumor-infiltrating immune cells. TMZ alone significantly reduced NK and CD4 T cells, and IR as well as the combination of TMZ and IR reduced NK cells within the tumor microenvironment (Fig. 6D). There was no difference in the composition of tumor-infiltrating immune cells in NKG2D$^{-/-}$ vs. NKG2D-intact mice. However, the activation status of infiltrating immune cells, which did not differ in untreated NKG2D$^{-/-}$ or NKG2D-intact mice, was impaired in NKG2D$^{-/-}$ mice upon treatment. NK cells as well as CD4 and CD8 T cells produced more IFNγ in NKG2D-intact mice following treatment with TMZ, IR, or the combination of TMZ and IR, and this induction was attenuated in NKG2D$^{-/-}$ mice. In NKG2D-intact mice, γδ T cells produced more IFNγ upon treatment with TMZ, IR, or the combination of TMZ and

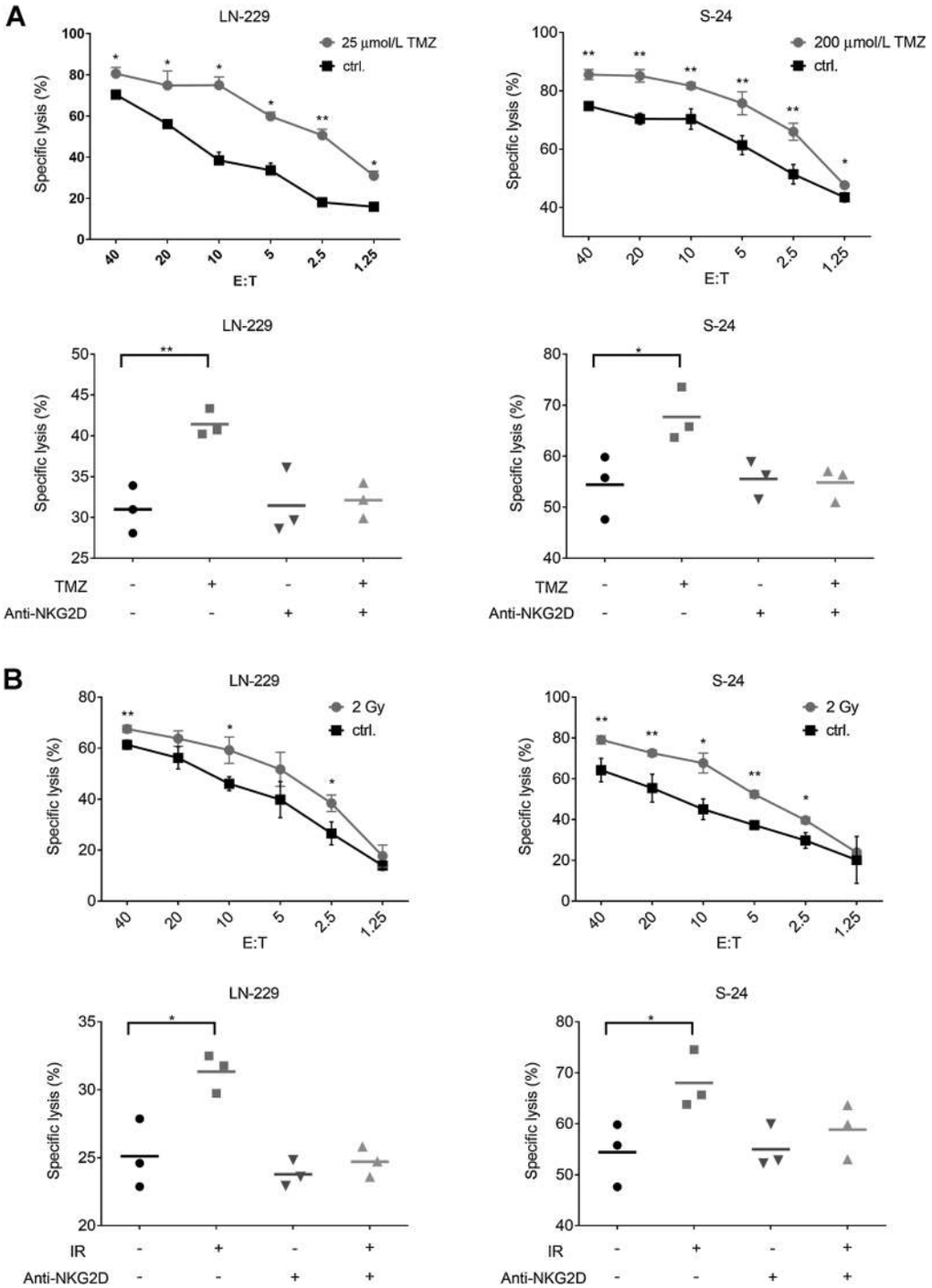

Figure 4.

Exposure to TMZ or IR promotes glioma cell immunogenicity in an NKG2D-dependent manner. **A,** Top: LN-229 (left) or S-24 (right) cells, preexposed to TMZ (gray line) or DMSO control (black line) for 48 hours, were used as target cells in a 3-hour immune cell lysis assays using polyclonal NK (for LN-229) or NKL (for S-24) effector cells at various effector:target (E:T) ratios. Following TMZ treatment, viable glioma cells were counted before coincubation with effector cells and immune-mediated cytolysis was corrected for spontaneous background lysis. Bottom, NKL cells were preincubated with anti-NKG2D antibody or isotype control and subsequently used as effector cells in lysis assays with LN-229 or S-24 glioma cells, either preexposed to TMZ or DMSO control, at an E:T ratio of 20:1. **B,** LN-229 or S-24 cells were irradiated with 2 Gy prior to use as target cells in 3-hour lysis assays. The experimental setup was the same as in **A**. In all figures, mean ± SD of triplicates from 1 representative out of 2 independent experiments is shown (*, $P < 0.05$; **, $P < 0.01$).

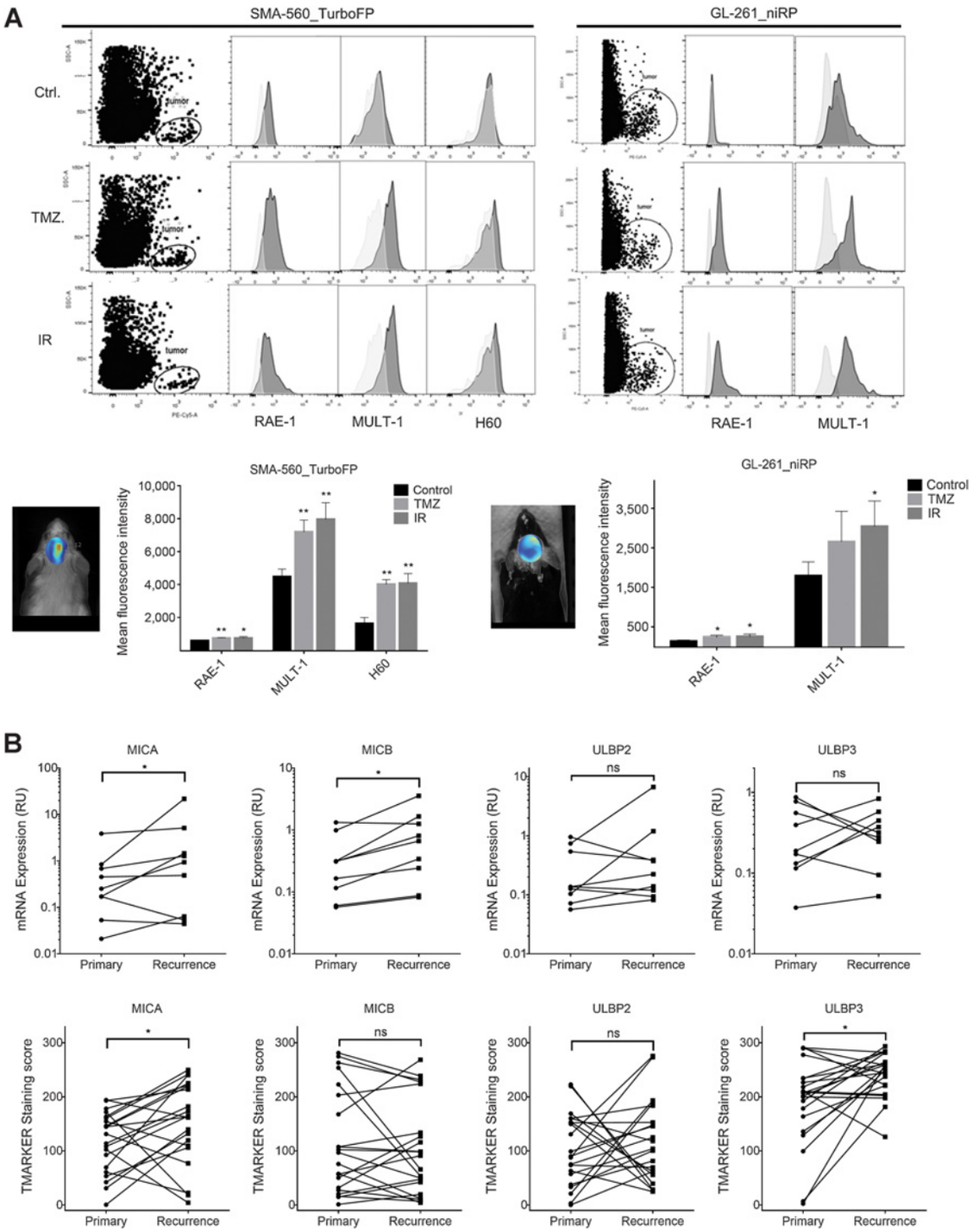

Figure 5.

TMZ and IR induce NKG2DL *in vivo* in syngeneic glioma models, and human glioblastoma patients have increased tumor-associated NKG2DL after radiochemotherapy. **A,** Orthotopic tumor-bearing mice [SMA-560_TurboFP in VM/Dk mice (left) or GL-261_niRP in C57BL/6 mice (right)] received a single dose of local irradiation (12 Gy) on day 10 or TMZ (10 mg/kg/day) per oral gavage from days 7 to 11 after tumor implantation. Mice were sacrificed on day 12, tumors were dissociated and cells analyzed for NKG2DL cell surface expression by flow cytometry. Tumor cells were gated in the dot plot diagrams based on the fluorescent signal. Histograms represent mean fluorescence intensity of RAE-1, MULT-1, and H60 on these cells. The diagrams summarize results of 5 mice per group. Data are presented as mean fluorescence intensity ± SD (*, $P < 0.05$; **, $P < 0.01$). **B,** NKG2DL were assessed on mRNA (top) and surface protein level (bottom) in matched pairs of human primary and recurrent tumors. Positive cell surface staining events were quantified in an unsupervised fashion with the TMARKER toolkit. (*, $P < 0.05$; ns = non-significant).

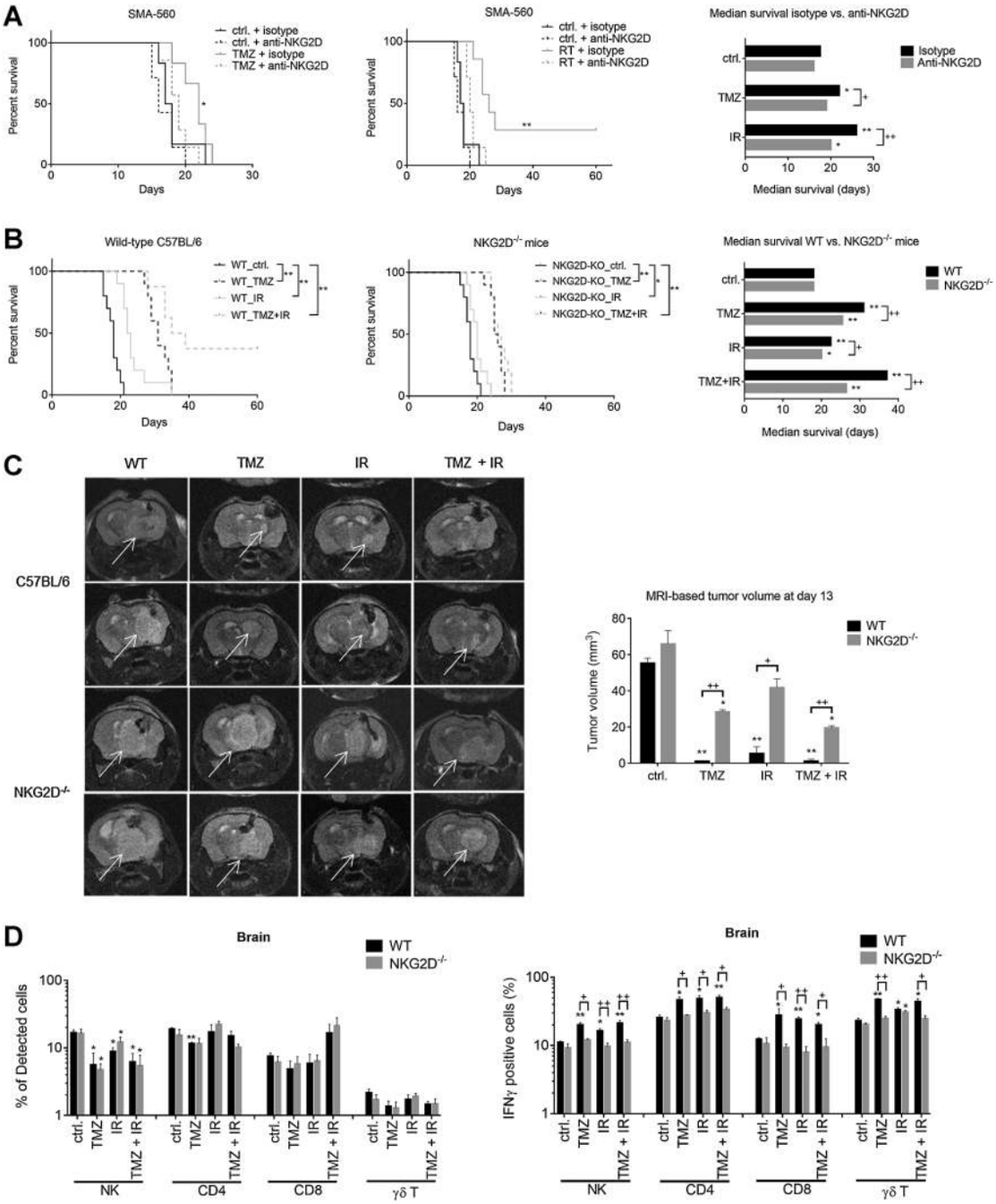

Figure 6.

The NKG2D system contributes to the therapeutic effects of TMZ and IR in glioma. **A,** SMA-560 tumor-bearing mice received injections of anti-NKG2D or isotype control antibody 1 day before and 1 day and then every 7 days after tumor implantation. Subsequently, the animals were treated with TMZ or solvent control from days 7 to 11 or a single dose of IR at day 12. Survival data are presented as Kaplan–Meier plots (left and center). Combined analysis of median survival is plotted on the right. Survival differences were compared between different treatment groups (*, $P < 0.05$; **, $P < 0.01$) and within a treatment group between isotype or anti-NKG2D treatment (+, $P < 0.05$; ++, $P < 0.01$). **B–D,** GL-261 tumor–bearing C57BL/6 or NKG2D$^{-/-}$ mice were treated with IR (single local dose of 12 Gy at day 10), TMZ (10 mg/kg p.o., days 7–11) or the combination of both. **B,** Survival data are presented as Kaplan–Meier plots (left and center). Combined analysis of median survival of the different groups is plotted on the right (*, $P < 0.05$; **, $P < 0.01$ between treatment groups and +, $P < 0.05$; ++, $P < 0.01$ within a treatment group for intact NKG2D vs. NKG2D$^{-/-}$). **C,** T2-weighted coronal scans were acquired at day 13 after tumor implantation. Two representative scans for each group are shown (left). The white arrow marks the tumor region. Mean ± SD of the tumor volume in mm^3 from 4 mice/group is shown (right). **D,** Percentage of NK, CD4, CD8, and γδ T cells (left) and the corresponding IFNγ secretion (right) of tumor-infiltrating lymphocytes derived from mice described in **B** and **C** were determined at day 14 after tumor implantation. Mean ± SD from 3 mice is shown (*, $P < 0.05$; **, $P < 0.01$ between treatment groups and +, $P < 0.05$; ++, $P < 0.01$ within a treatment group for intact NKG2D vs. NKG2D$^{-/-}$).

IR compared with NKG2D$^{-/-}$ mice. In NKG2D$^{-/-}$ mice, we observed more IFNγ production in γδ T cells only upon IR (Fig. 6D; Supplementary Fig. S6D–S6F).

Discussion

TMZ chemotherapy and radiotherapy constitute the standard treatment modalities in patients with newly diagnosed glioblastoma (43). The antiglioma effects of TMZ and IR comprise different molecular mechanisms such as induction of cell-cycle arrest, senescence, and apoptosis (47, 48). Furthermore, there is increasing evidence that cell death upon exposure to TMZ or IR can promote antitumor immune responses by releasing tumor-associated antigens or damage-associated molecular pattern molecules such as calreticulin, adenosine triphosphate, or high-mobility group box 1 protein (49–51). In addition to these soluble and potentially immune-stimulating molecules, glioma cells express membrane-bound ligands to the activating immune cell receptor NKG2D which basically enables target cell killing without prior sensitization and irrespective of MHC restriction.

We observed an upregulation of several NKG2DL on mRNA and protein level upon exposure to TMZ, CCNU, or IR in several mouse and human glioma cells, including stem-like cells (Figs. 1 and 2; Supplementary Figs. S1 and S2). NKG2DL induction by TMZ has previously been reported in four other human glioma cell lines (52). We found that the NKG2DL induction was independent from cytotoxic or growth inhibitory effects and was achieved at clinically relevant concentrations of chemotherapeutic agents and low doses of IR. Furthermore, we confirmed the upregulation of NKG2DL on glioma cells upon treatment with TMZ or IR *in vivo* in two orthotopic mouse glioma models (Fig. 5A). The use of fluorescently labeled glioma cells excluded contaminating signals from immune cells which could also express NKG2DL (53). These findings were further corroborated by an analysis of paired samples of human glioblastoma tissue specimens obtained from patients during initial surgery and at tumor recurrence following radio- and/or chemotherapy. The increased NKG2DL expression levels after alkylating chemotherapy or radiotherapy support our *in vitro* data as well as findings from the mouse studies (Fig. 5B). Changes in glioma cell NKG2DL levels may be confounded by other factors than treatment such as passenger mutations that occur during the course of the disease (54, 55). Despite these limitations, our data strongly suggest that NKG2DL expression levels are increased following radiochemotherapy. Together with the observation that NKG2DL can also be induced in TMZ-resistant cells (Supplementary Fig. S3C and S3D), this provides a rationale to investigate NKG2D-targeting therapies (27) also at tumor recurrence.

We demonstrate that the upregulation of NKG2DL upon TMZ or IR requires ATM (Fig. 3D; Supplementary Fig. S3G), which supports the concept that the DNA-damage response is one stimulus for the induction of NKG2DL (56). Consequently, ATM inhibitors may potentially counteract NKG2D-dependent antitumor immune effects. This needs to be considered in future trials evaluating the activity of such ATM inhibitors as radiosensitizers (57).

Although the net effect of NKG2D ligand induction is of rather small magnitude, it has important functional consequences. The induction of NKG2DL by TMZ or IR enhanced the immunogenicity of glioma cells, including GIC, and rendered the cells more susceptible to immune-mediated cytolysis (Fig. 4; Supplementary Fig. S4A). Chemotherapy and radiotherapy have various effects on tumor cells and the microenvironment comprising both immune-stimulatory and immune-suppressive mechanisms. Our study indicates that treatment-associated NKG2DL induction constitutes a relevant immune-stimulatory mechanism because inhibition of NKG2D signaling abrogated the enhanced cytolysis. Furthermore, tumor-infiltrating NK, CD4, CD8 T cells and to some extent also γδ T cells produced more IFNγ in an NKG2D-dependent manner upon treatment with TMZ and/or irradiation (Fig. 6D). This emphasizes the relevance of the NKG2D-mediated immune-stimulatory mechanism of TMZ and IR and adds another relevant mechanism to the concept of immunogenic cell death.

We did not only demonstrate that TMZ- and radiotherapy-mediated NKG2DL induction can be used as a strategy to render glioma cells more immunogenic but also that the full efficacy of TMZ and IR against glioblastoma depends on an intact NKG2D system. The survival benefit gained with these treatment modalities was diminished upon blockade of NKG2D signaling with an inhibitory but nondepleting antibody or in NKG2D knockout mice (Fig. 6A and B; Supplementary Fig. S6A–S6C). Inhibition or deficiency of NKG2D in mice did not result in a significant survival difference without additional treatment, suggesting that the basal expression levels of NKG2DL are too low to promote a relevant immune response (7, 10, 26, 34, 58).

The NKG2DL induction upon TMZ treatment or IR could provide a rationale for future studies investigating the synergistic application of these conventional treatment modalities with other NKG2D-based immunotherapeutic strategies (27). So far, one phase I study has used pure NK cells for adoptive immunotherapy in patients with recurrent malignant gliomas (59). However, no concomitant treatment with TMZ or IR was administered and additive or synergistic effects to this adoptive cell therapy need to be explored in future clinical trials.

In summary, the present dataset demonstrates the relevance of a so far unrecognized mechanism mediating antitumor effects of TMZ and IR that is likely to be clinically relevant. Based on our findings, further studies evaluating the combination of radiochemotherapy with additional NKG2D-based immunotherapeutic strategies should be considered for the treatment of glioblastoma.

Disclosure of Potential Conflicts of Interest

P. Roth reports receiving speakers bureau honoraria from BMS, Novartis, and Novocure, and is a consultant/advisory board member for MSD, Roche, Virometix, Covagen, and Molecular Partners. No potential conflicts of interest were disclosed by the other authors.

Authors' Contributions

Conception and design: T. Weiss, M. Weller, P. Roth
Development of methodology: T. Weiss, M. Pruschy, P. Roth
Acquisition of data (provided animals, acquired and managed patients, provided facilities, etc.): T. Weiss, H. Schneider, M. Silginer, M. Pruschy, B. Polić
Analysis and interpretation of data (e.g., statistical analysis, biostatistics, computational analysis): T. Weiss, M. Pruschy, M. Weller
Writing, review, and/or revision of the manuscript: T. Weiss, H. Schneider, A. Steinle, M. Pruschy, B. Polić, M. Weller, P. Roth

Administrative, technical, or material support (i.e., reporting or organizing data, constructing databases): T. Weiss, A. Steinle, M. Weller, P. Roth
Study supervision: T. Weiss, M. Weller, P. Roth

Acknowledgments

This study was supported by grants from the Gertrud-Hagmann Foundation and the Swiss Cancer League (KFS-3478-08-2014) to P. Roth and "Hochspezialisierte Medizin Zurich" (HSM-2) to M. Weller and P. Roth.

The costs of publication of this article were defrayed in part by the payment of page charges. This article must therefore be hereby marked *advertisement* in accordance with 18 U.S.C. Section 1734 solely to indicate this fact.

Received June 20, 2017; revised October 12, 2017; accepted November 15, 2017; published OnlineFirst November 21, 2017.

References

1. Weller M, Wick W, Aldape KD, Brada M, Berger SM, Nishikawa R, et al. Glioma. Nat Rev Dis Primers 2015:15017.
2. Stupp R, Mason WP, van den Bent MJ, Weller M, Fisher B, Taphoorn MJB, et al. Radiotherapy plus concomitant and adjuvant temozolomide for glioblastoma. N Engl J Med 2005;352:987–96.
3. Weller M, van den Bent M, Tonn JC, Stupp R, Preusser M, Cohen-Jonathan-Moyal E, et al. European Association for Neuro-Oncology (EANO) guideline on the diagnosis and treatment of adult astrocytic and oligodendroglial gliomas. Lancet Oncol 2017;18:e315–e29.
4. Preusser M, Lim M, Hafler DA, Reardon DA, Sampson JH. Prospects of immune checkpoint modulators in the treatment of glioblastoma. Nat Rev Neurol 2015;11:504–14.
5. Weiss T, Weller M, Roth P. Immunotherapy for glioblastoma: concepts and challenges. Curr Opin Neurol 2015;28:639–46.
6. Dutoit V, Herold-Mende C, Hilf N, Schoor O, Beckhove P, Bucher J, et al. Exploiting the glioblastoma peptidome to discover novel tumour-associated antigens for immunotherapy. Brain 2012;135:1042–54.
7. Crane CA, Han SJ, Barry JJ, Ahn BJ, Lanier LL, Parsa AT. TGF-beta downregulates the activating receptor NKG2D on NK cells and CD8+ T cells in glioma patients. Neuro Oncol 2010;12:7–13.
8. Raulet DH, Gasser S, Gowen BG, Deng W, Jung H. Regulation of ligands for the NKG2D activating receptor. Annu Rev Immunol 2013;31:413–41.
9. Friese MA, Platten M, Lutz SZ, Naumann U, Aulwurm S, Bischof F, et al. MICA/NKG2D-mediated immunogene therapy of experimental gliomas. Cancer Res 2003;63:8996–9006.
10. Eisele G, Wischhusen J, Mittelbronn M, Meyermann R, Waldhauer I, Steinle A, et al. TGF-beta and metalloproteinases differentially suppress NKG2D ligand surface expression on malignant glioma cells. Brain 2006;129:2416–25.
11. Di Tomaso T, Mazzoleni S, Wang E, Sovena G, Clavenna D, Franzin A, et al. Immunobiological characterization of cancer stem cells isolated from glioblastoma patients. Clin Cancer Res 2010;16:800–13.
12. Wolpert F, Tritschler I, Steinle A, Weller M, Eisele G. A disintegrin and metalloproteinases 10 and 17 modulate the immunogenicity of glioblastoma-initiating cells. Neuro Oncol 2014;16:382–91.
13. Beck BH, Kim H, O'Brien R, Jadus MR, Gillespie GY, Cloud GA, et al. Dynamics of circulating gammadelta T cell activity in an immunocompetent mouse model of high-grade glioma. PloS One 2015;10:e0122387.
14. Bauer S, Groh V, Wu J, Steinle A, Phillips JH, Lanier LL, et al. Activation of NK cells and T cells by NKG2D, a receptor for stress-inducible MICA. Science 1999;285:727–9.
15. Groh V, Bruhl A, El-Gabalawy H, Nelson JL, Spies T. Stimulation of T cell autoreactivity by anomalous expression of NKG2D and its MIC ligands in rheumatoid arthritis. Proc Nat Acad Sci U S A 2003;100:9452–7.
16. Sanchez-Correa B, Morgado S, Gayoso I, Bergua JM, Casado JG, Arcos MJ, et al. Human NK cells in acute myeloid leukaemia patients: analysis of NK cell-activating receptors and their ligands. Cancer Immunol Immunother 2011;60:1195–205.
17. Frei K, Gramatzki D, Tritschler I, Schroeder JJ, Espinoza L, Rushing EJ, et al. Transforming growth factor-beta pathway activity in glioblastoma. Oncotarget 2015;6:5963–77.
18. Sawamura Y, Diserens AC, de Tribolet N. In vitro prostaglandin E2 production by glioblastoma cells and its effect on interleukin-2 activation of oncolytic lymphocytes. J Neuro-Oncol 1990;9:125–30.
19. Huettner C, Paulus W, Roggendorf W. Messenger RNA expression of the immunosuppressive cytokine IL-10 in human gliomas. Am J Pathol 1995;146:317–22.
20. Roth P, Junker M, Tritschler I, Mittelbronn M, Dombrowski Y, Breit SN, et al. GDF-15 contributes to proliferation and immune escape of malignant gliomas. Clin Cancer Res 2010;16:3851–9.
21. Roth P, Mittelbronn M, Wick W, Meyermann R, Tatagiba M, Weller M. Malignant glioma cells counteract antitumor immune responses through expression of lectin-like transcript-1. Cancer Res 2007;67:3540–4.
22. Miyazaki T, Moritake K, Yamada K, Hara N, Osago H, Shibata T, et al. Indoleamine 2,3-dioxygenase as a new target for malignant glioma therapy. Laboratory investigation. J Neurosurg 2009;111:230–7.
23. Berghoff AS, Kiesel B, Widhalm G, Rajky O, Ricken G, Wohrer A, et al. Programmed death ligand 1 expression and tumor-infiltrating lymphocytes in glioblastoma. Neuro Oncol 2015;17:1064–75.
24. Tran Thang NN, Derouazi M, Philippin G, Arcidiaco S, Di Berardino-Besson W, Masson F, et al. Immune infiltration of spontaneous mouse astrocytomas is dominated by immunosuppressive cells from early stages of tumor development. Cancer Res 2010;70:4829–39.
25. Zhou W, Ke SQ, Huang Z, Flavahan W, Fang X, Paul J, et al. Periostin secreted by glioblastoma stem cells recruits M2 tumour-associated macrophages and promotes malignant growth. Nat Cell Biol 2015;17:170–82.
26. Friese MA, Wischhusen J, Wick W, Weiler M, Eisele G, Steinle A, et al. RNA interference targeting transforming growth factor-beta enhances NKG2D-mediated antiglioma immune response, inhibits glioma cell migration and invasiveness, and abrogates tumorigenicity in vivo. Cancer Res 2004;64:7596–603.
27. Spear P, Wu MR, Sentman ML, Sentman CL. NKG2D ligands as therapeutic targets. Cancer Immun 2013;13:8.
28. Happold C, Roth P, Wick W, Schmidt N, Florea AM, Silginer M, et al. Distinct molecular mechanisms of acquired resistance to temozolomide in glioblastoma cells. J Neurochem 2012;122:444–55.
29. Hermisson M, Klumpp A, Wick W, Wischhusen J, Nagel G, Roos W, et al. O6-methylguanine DNA methyltransferase and p53 status predict temozolomide sensitivity in human malignant glioma cells. J Neurochem 2006;96:766–76.
30. Maurer GD, Tritschler I, Adams B, Tabatabai G, Wick W, Stupp R, et al. Cilengitide modulates attachment and viability of human glioma cells, but not sensitivity to irradiation or temozolomide in vitro. Neuro Oncol 2009;11:747–56.
31. Silginer M, Nagy S, Happold C, Schneider H, Weller M, Roth P. Autocrine activation of the IFN signaling pathway may promote immune escape in glioblastoma. Neuro Oncol 2017;19:1338–49.
32. Fowler JF. The linear-quadratic formula and progress in fractionated radiotherapy. Br J Radiol 1989;62:679–94.
33. Salih HR, Antropius H, Gieseke F, Lutz SZ, Kanz L, Rammensee HG, et al. Functional expression and release of ligands for the activating immunoreceptor NKG2D in leukemia. Blood 2003;102:1389–96.
34. Codo P, Weller M, Meister G, Szabo E, Steinle A, Wolter M, et al. MicroRNA-mediated down-regulation of NKG2D ligands contributes to glioma immune escape. Oncotarget 2014;5:7651–62.
35. Welte SA, Sinzger C, Lutz SZ, Singh-Jasuja H, Sampaio KL, Eknigk U, et al. Selective intracellular retention of virally induced NKG2D ligands by the human cytomegalovirus UL16 glycoprotein. Eur J Immunol 2003;33:194–203.
36. Zafirova B, Mandaric S, Antulov R, Krmpotic A, Jonsson H, Yokoyama WM, et al. Altered NK cell development and enhanced NK cell-mediated resistance to mouse cytomegalovirus in NKG2D-deficient mice. Immunity 2009;31:270–82.
37. Smyth MJ, Swann J, Kelly JM, Cretney E, Yokoyama WM, Diefenbach A, et al. NKG2D recognition and perforin effector function mediate effective cytokine immunotherapy of cancer. J Exp Med 2004;200:1325–35.

38. Schuffler PJ, Fuchs TJ, Ong CS, Wild PJ, Rupp NJ, Buhmann JM. TMARKER: a free software toolkit for histopathological cell counting and staining estimation. J Pathol Inform 2013;4:S2.
39. Pohl M, Olsen KE, Holst R, Ditzel HJ, Hansen O. Tissue microarrays in non-small-cell lung cancer: reliability of immunohistochemically-determined biomarkers. Clin Lung Cancer 2014;15:222–30e3.
40. Hammond LA, Eckardt JR, Baker SD, Eckhardt SG, Dugan M, Forral K, et al. Phase I and pharmacokinetic study of temozolomide on a daily-for-5-days schedule in patients with advanced solid malignancies. J Clin Oncol 1999; 17:2604–13.
41. Eyler CE, Rich JN. Survival of the fittest: cancer stem cells in therapeutic resistance and angiogenesis. J Clin Oncol 2008;26:2839–45.
42. Takada A, Yoshida S, Kajikawa M, Miyatake Y, Tomaru U, Sakai M, et al. Two novel NKG2D ligands of the mouse H60 family with differential expression patterns and binding affinities to NKG2D. J Immunol 2008; 180:1678–85.
43. Weller M, van den Bent M, Hopkins K, Tonn JC, Stupp R, Falini A, et al. EANO guideline for the diagnosis and treatment of anaplastic gliomas and glioblastoma. Lancet Oncol 2014;15:e395–403.
44. Lee FY, Workman P, Roberts JT, Bleehen NM. Clinical pharmacokinetics of oral CCNU (lomustine). Cancer Chemother Pharmacol 1985;14:125–31.
45. Caporali S, Falcinelli S, Starace G, Russo MT, Bonmassar E, Jiricny J, et al. DNA damage induced by temozolomide signals to both ATM and ATR: role of the mismatch repair system. Mol Pharmacol 2004;66:478–91.
46. Robertson MJ, Cochran KJ, Cameron C, Le JM, Tantravahi R, Ritz J. Characterization of a cell line, NKL, derived from an aggressive human natural killer cell leukemia. Exp Hematol 1996;24:406–15.
47. Eriksson D, Stigbrand T. Radiation-induced cell death mechanisms. Tumour Biol 2010;31:363–72.
48. Knizhnik AV, Roos WP, Nikolova T, Quiros S, Tomaszowski KH, Christmann M, et al. Survival and death strategies in glioma cells: autophagy, senescence and apoptosis triggered by a single type of temozolomide-induced DNA damage. PLoS One 2013;8:e55665.
49. Krysko O, Love Aaes T, Bachert C, Vandenabeele P, Krysko DV. Many faces of DAMPs in cancer therapy. Cell Death Dis 2013;4:e631.
50. Paolini A, Pasi F, Facoetti A, Mazzini G, Corbella F, Di Liberto R, et al. Cell death forms and HSP70 expression in U87 cells after ionizing radiation and/or chemotherapy. Anticancer Res 2011;31:3727–31.
51. Rubner Y, Muth C, Strnad A, Derer A, Sieber R, Buslei R, et al. Fractionated radiotherapy is the main stimulus for the induction of cell death and of Hsp70 release of p53 mutated glioblastoma cell lines. Radiation Oncol 2014;9:89.
52. Chitadze G, Lettau M, Luecke S, Wang T, Janssen O, Furst D, et al. NKG2D- and T-cell receptor-dependent lysis of malignant glioma cell lines by human gammadelta T cells: modulation by temozolomide and A disintegrin and metalloproteases 10 and 17 inhibitors. Oncoimmunology 2016;5:e1093276.
53. Cerboni C, Zingoni A, Cippitelli M, Piccoli M, Frati L, Santoni A. Antigen-activated human T lymphocytes express cell-surface NKG2D ligands via an ATM/ATR-dependent mechanism and become susceptible to autologous NK- cell lysis. Blood 2007;110:606–15.
54. Ho SS, Gasser S. NKG2D ligands link oncogenic RAS to innate immunity. Oncoimmunology 2013;2:e22244.
55. Wang J, Cazzato E, Ladewig E, Frattini V, Rosenbloom DI, Zairis S, et al. Clonal evolution of glioblastoma under therapy. Nat Genet 2016;48: 768–76.
56. Gasser S, Orsulic S, Brown EJ, Raulet DH. The DNA damage pathway regulates innate immune system ligands of the NKG2D receptor. Nature 2005;436:1186–90.
57. Biddlestone-Thorpe L, Sajjad M, Rosenberg E, Beckta JM, Valerie NC, Tokarz M, et al. ATM kinase inhibition preferentially sensitizes p53-mutant glioma to ionizing radiation. Clin Cancer Res 2013;19: 3189–200.
58. Crane CA, Austgen K, Haberthur K, Hofmann C, Moyes KW, Avanesyan L, et al. Immune evasion mediated by tumor-derived lactate dehydrogenase induction of NKG2D ligands on myeloid cells in glioblastoma patients. Proc Nat Acad Sci U S A 2014;111:12823–8.
59. Ishikawa E, Tsuboi K, Saijo K, Harada H, Takano S, Nose T, et al. Autologous natural killer cell therapy for human recurrent malignant glioma. Anticancer Res 2004;24:1861–71.